

# NUMERICAL SIMULATION OF A FLOW OVER A CYLINDER WITH IMMERSED BOUNDARY TECHNIQUE IN VORTICITY-VELOCITY FORMULATION

Evelise Roman Corbalan Góis, [evelise@icmc.usp.br](mailto:evelise@icmc.usp.br)

Leandro Franco de Souza, [lefraso@icmc.usp.br](mailto:lefraso@icmc.usp.br)

Departamento de Matemática Aplicada e Estatística-ICMC (USP)

CEP – 13560-970 – São Carlos – SP – Brazil

## Abstract.

*The study of vortex shedding in the flow over obstacles is crucial to a variety of engineering problems. However, it is very hard to perform computational simulations of these phenomena due to the computational effort. In this paper, we describe the use of an Immersed Boundary Method, to simulate the flow over an oscillating cylinder with low Reynolds number. The main idea of this method is to transfer the fluid's properties in the cylinder's boundary directly to the mesh, what enables the use of regular meshes, reducing the computational effort. The governing equations were written in vorticity-velocity formulation. The spatial derivatives were calculated by high order finite difference schemes. The time integration was performed by a fourth order Runge-Kutta scheme. A control volume was implemented and the lift and drag coefficients obtained were compared with the forcing terms of the governing equations. The results obtained were in good agreement with previous numerical / experimental works.*

**Keywords:** Immersed Boundary Method, low Reynolds number, forcing terms, vorticity-velocity formulation, lift and drag coefficients.

## 1. INTRODUCTION

The understanding of the characteristics of flow over obstacles is of great importance in engineering applications. However, performing these computational simulations can be very hard due to the computational effort required by the use of irregular meshes. A solution for this problem is the use of the Immersed Boundary Method, that requires a fixed Cartesian mesh instead of a conforming mesh. In this method a forcing term is added to the governing equations. The Immersed Boundary Method's founding father is Peskin (1972), who developed the technique to study blood flow in human heart valves. The information about the boundary position and the elastic force is transferred to the Cartesian mesh in order to obtain a flow solution.

The flow over a circular cylinder has been studied by a number of authors. Braza, Chassaing and Minh (1986) investigated the interaction between the pressure and velocity fields in the flow over a circular cylinder. The Navier-Stokes equations were solved by a predictor-corrector pressure implicit procedure. They performed simulations for Reynolds-number values of 20, 40, 100, 200 and 1000 and the drag and lift coefficients were evaluated. The vortex shedding was generated by a physical perturbation imposed numerically. For  $Re = 20$  e  $Re = 40$  two attached vortices were formed behind the cylinder. For  $Re = 20$  the drag coefficient  $C_d$  were between 1.8 and 2.4. For  $Re = 40$ , the lift coefficient value  $C_l$  were between 1.4 and 1.8. For others Reynolds values, the perturbations introduced correspond to a clockwise rotation of the cylinder followed by a counterclockwise rotation. They found a phase opposition of the pressure relative to the velocity inside and outside the wake.

Góis and Souza (2006) have accomplished a numerical simulation of the flow over a steady cylinder with variation in the inflow velocity and over an oscillating cylinder with constant velocity inflow. The Reynolds number adopted was  $Re = 185$ . The oscillation frequency was  $\omega = 0.9$  and the amplitude oscillation was  $A = 0.2$ . The results for the cylinder oscillating with inflow velocity constant were in good agreement with the case with the stationary cylinder with velocity inflow variation. These results were compared with experimental results from Gu, Chyu and Rockwell (1994), validating their code.

Góis and Souza (2007) studied the Lock-in phenomena of the fluid flow over a cylinder of circular section. This study was based on a two-dimensional simulation of the fluid flow with low Reynolds numbers over a cylinder that may be stationary or periodically moved with given frequency and amplitude. The objective was to capture the Lock-in phenomena. The Lock-in Phenomena occur when the obstacle oscillates with a given frequency and amplitude and the flow can be influenced by this oscillation. These phenomena are of particular interest and were discovered over three hundred years ago when Christian Huygens observed that two pendula placed next to each other had a tendency to synchronize their movements. For  $Re = 190$ , they tested different values of oscillations frequency  $\omega$ :  $\omega = 0.5$ ,  $\omega = 1.5$ ,  $\omega = 2.0$  and  $\omega = 3.0$ . The Lock-in phenomena were captured for frequencies  $F = 1.5$  and  $F = 2.0$ . These numerical results of lock-in phenomena agree with experimental results from Griffin and Ramberg (1976).

The purpose of the work reported in this paper is to study the 2D unsteady flow over a stationary or moving periodically

circular cylinder at low Reynolds. It is studied the drag and lift coefficients, respectively  $C_d$  and  $C_l$ . The simulations were performed for  $Re = 20$ ,  $Re = 40$  and  $Re = 190$ . The cylinder can be either oscillatory or stationary. The results were validated and verified, with good agreements with the literature.

## 2. METHODS

### 2.1 The Governing Equations and Immersed Boundary Method

In this study, the governing equations are the incompressible, unsteady Navier-Stokes equations with constant density and viscosity. They consist of the momentum equations for the velocity components ( $u, v$ ), given by:

$$\frac{\partial u}{\partial t} + u \frac{\partial u}{\partial x} + v \frac{\partial u}{\partial y} = -\frac{\partial p}{\partial x} + \nabla^2 u + F_x, \quad (1)$$

$$\frac{\partial v}{\partial t} + u \frac{\partial v}{\partial x} + v \frac{\partial v}{\partial y} = -\frac{\partial p}{\partial y} + \nabla^2 v + F_y, \quad (2)$$

and the continuity equation:

$$\frac{\partial u}{\partial x} + \frac{\partial v}{\partial y} = 0, \quad (3)$$

where  $u$  is the velocity component in the streamwise direction  $x$ ,  $v$  is the component velocity in the streamwise normal direction  $y$ ,  $\rho$  is the density,  $p$  is the pressure,  $\nabla$  is given by:

$$\nabla = \frac{1}{Re} \left( \frac{\partial^2}{\partial x^2} + \frac{\partial^2}{\partial y^2} \right), \quad (4)$$

and  $F_x$  and  $F_y$  are the forcing terms used by the immersed boundary technique.

The vorticity is here defined as the negative curl of velocity vector. Taking the curl of the momentum equations, the vorticity transport equation can be obtained:

$$\frac{\partial \omega_z}{\partial t} = -u \frac{\partial \omega_z}{\partial x} - v \frac{\partial \omega_z}{\partial y} + \nabla^2 \omega_z + \frac{\partial F_x}{\partial y} - \frac{\partial F_y}{\partial x}. \quad (5)$$

From the definition of vorticity and the continuity equation, the Poisson equation for  $v$  velocity component can be obtained:

$$\frac{\partial v^2}{\partial x^2} + \frac{\partial v^2}{\partial y^2} = -\frac{\partial \omega_z}{\partial x}. \quad (6)$$

The boundary conditions adopted are: at the inflow boundary in the integration domain ( $x = x_0$ ), the velocity and vorticity components are specified. At the outflow boundary ( $x = x_{max}$ ), the second derivative of the velocity and vorticity components in the streamwise direction are set to zero. At the upper ( $y = y_{max}$ ) and lower ( $y = 0$ ) boundaries, the derivatives of  $v$  in the  $y$  direction are set to zero.

Three damping zones were used in the simulations to force the disturbances to gradually decay to zero. The basic idea is to multiply the vorticity components by a ramp function  $f_2(x)$  after each step of the integration scheme. This technique has been proved by Kloker (1998) to be very efficient in avoiding reflections that could come from the boundaries when simulating flows with disturbances. Using this technique, the vorticity components are taken as:

$$\omega_z(x, y) = f_2(x)\omega(x, y, t) \quad (7)$$

where  $\omega(x, y, t)$  is the disturbance vorticity component that comes out from the time integration scheme and  $f_2(x)$  is a ramp function that goes smoothly from 1 to 0. The implemented function, in the  $x$  direction, was:

$$f_2(x) = f(\epsilon) = 1 - 6\epsilon^5 + 15\epsilon^4 - 10\epsilon^3 \quad (8)$$

where  $\epsilon = \frac{(i-i_3)}{i_4-i_3}$  for  $i \leq i \leq i_4$  corresponds to the positions  $x_3$  and  $x_4$  in the streamwise direction respectively. To ensure good numerical results, a minimum distance between  $x_4$  and the end of domain  $x_{max}$  should be specified.

The spatial derivatives were calculated using a 6<sup>th</sup> order compact finite difference scheme (Souza et al. (2005)). The  $v$ -Poisson was solved using a Full Approximation Scheme (FAS) multigrid a v-cycle working with 4 grids. The forcing terms were calculated using the following equations:

$$F_x(i, j) = \delta fr(vel_u - vel_{cil}), \quad (9)$$

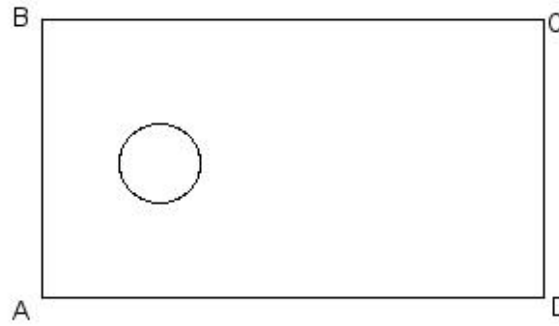


Figure 1. Control surface

$$F_y(i, j) = \delta fr(vel_v - vel_{cil}), \quad (10)$$

where  $fr$  is the relaxation term, here  $fr = -300$ ,  $u$  and  $v$  are the velocity components in the streamwise and normal directions respectively and  $\delta$  is a value that varies from  $\delta(i, j) = 0$  outside the immersed body to  $\delta(i, j) = 1$  at the boundary and inside the immersed body. In the case for stationary cylinder,  $vel_{cil} = 0$ .

The time integration is calculated using a fourth-order Runge-Kutta scheme, and the numerical procedure works as described next. At each step of the Runge-Kutta scheme the following instructions are necessary:

1. Compute the spatial derivatives of the vorticity transport equation;
2. Calculate the forcing terms  $F_x$  and  $F_y$ ;
3. Calculate the rotational of the forcing terms;
4. Integrate the vorticity transport equation over one step (or sub-step) of the scheme using the values obtained in steps 1 and 3;
5. Calculate  $v$  from the Poisson equation;
6. Calculate  $u$  from the continuity equation;
7. Verify the values of the velocity components at the immersed boundary, if they are below a predefined value continue, otherwise go to step 2

This scheme is repeated until a stable or a time periodic solution is reached. The next section shows the results obtained for steady or oscillating cylinder using the numerical code described here.

## 2.2 The Control Volume Method

The calculus of the drag and lift coefficients  $C_l$  and  $C_d$  were done by means of the Control Volume method. This method is based on the determination of an arbitrary volume in the space over which the fluid flows. The geometric boundary of the control volume is named "control surface". In this work, the control surface remains fixed around the cylinder, which is used as an obstacle to the flow. Figure 1 shows the adopted control surface.

The temporal term  $\frac{\partial}{\partial t}$ , the convective terms  $\vec{u} \nabla \vec{u}$ , the diffusive terms  $\nabla^2$  and the pressure terms  $P$  were implemented separately. The control volume was defined as a rectangular shape. The diffusive, convective, and pressure terms are calculated at each of the faces, and the integrals are solved using the trapezoidal rule.

To perform the computation in the control volume, the drag and the lift coefficients can be calculated as:

$$C_d = -2 \iint \left[ \frac{\partial u}{\partial t} + u \frac{\partial u}{\partial x} + v \frac{\partial u}{\partial y} + \frac{\partial p}{\partial x} - \frac{1}{Re} \left( \frac{\partial^2 u}{\partial x^2} + \frac{\partial^2 u}{\partial y^2} \right) \right] dx dy, \quad (11)$$

$$C_l = -2 \iint \left[ \frac{\partial v}{\partial t} + u \frac{\partial v}{\partial x} + v \frac{\partial v}{\partial y} + \frac{\partial p}{\partial y} - \frac{1}{Re} \left( \frac{\partial^2 v}{\partial x^2} + \frac{\partial^2 v}{\partial y^2} \right) \right] dx dy. \quad (12)$$

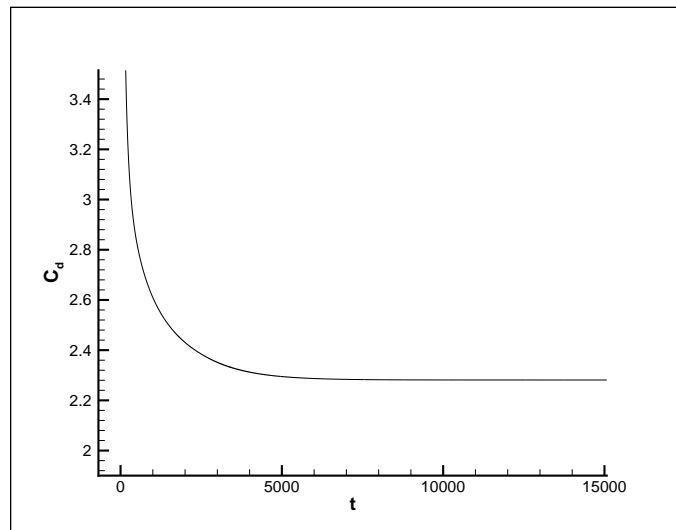


Figure 2. Drag coefficient for  $Re = 20$

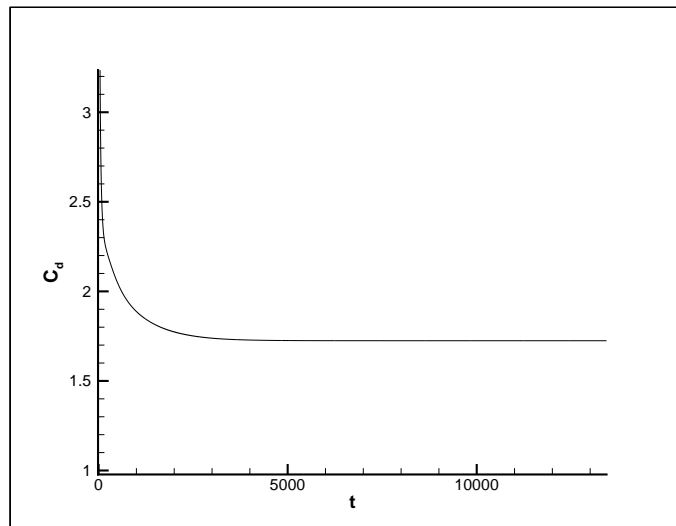


Figure 3. Drag coefficient for  $Re = 40$

### 3. RESULTS

The simulations were carried out with  $Re = 20$ ,  $Re = 40$  and  $Re = 190$ . The drag and lift coefficients  $C_l$  and  $C_d$  were evaluated. For  $Re = 20$ ,  $Re = 40$  the cylinder remained fixed in space. For  $Re = 190$ , the case with the cylinder oscillating in the flow direction was simulated. Four frequency oscillation values were tested, namely:  $\omega = 0.5$ ,  $\omega = 1.5$ ,  $\omega = 2.0$  and  $\omega = 3.0$ . Results obtained for the drag and lift coefficients were compared with the results obtained considering the forces from the fluid over the cylinder in x and y directions, namely  $F_x$  e  $F_y$ . These forces have the same intensity of the drag and lift coefficients, calculated using control volume techniques.

The graphs presented in Fig.2 and Fig.3 describe the behavior of  $C_d$  as function of non dimensional time for  $Re = 20$  and  $Re = 40$ , respectively. For  $Re = 20$  the value of drag coefficient was  $C_d = 2.28$  and for  $Re = 40$  the drag coefficient was  $C_d = 1.72$ . This results are in agreement with numerical and experimental results given by Braza, Chassaing and Minh (1986).

Figure 4 describes the vorticity contours of flow over a stationary cylinder for  $Re = 190$ . A simple vortex shedding occurs. Figure 5 shows the result obtained for the  $C_d$ ,  $F_x$ ,  $C_l$  and  $F_y$  with an stationed cylinder. It can be observed that the  $C_d$  and  $F_x$  give the same result while  $C_l$  and  $F_y$  showed some differences.

Figure 6 shows the vorticity contours for the simulation using  $Re = 190$  and frequency oscillation  $\omega = 0.5$ . The amplitude was  $A = 0.2$ . It can be verified in this figure that the vortex shedding is almost the same obtained with no oscillation. The result obtained for the  $C_d$ ,  $F_x$ ,  $C_l$  and  $F_y$  are shown in Fig. 7. Again, it can be observed that the  $C_d$  and  $F_x$  have the same result while  $C_l$  and  $F_y$  showed some differences.

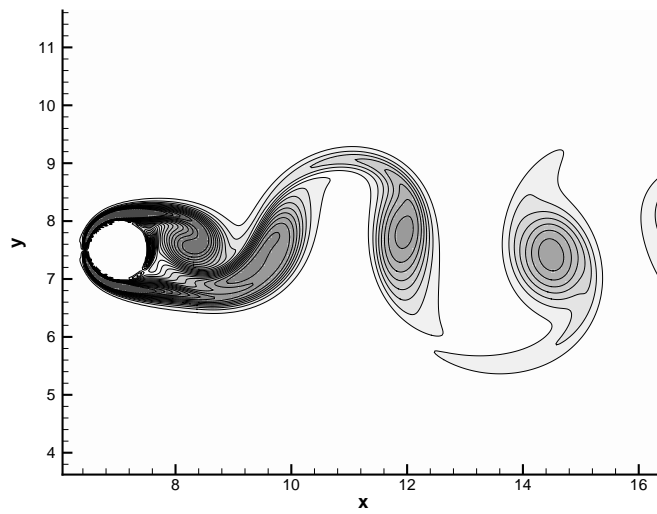


Figure 4. Vorticity contours with an stationed cylinder

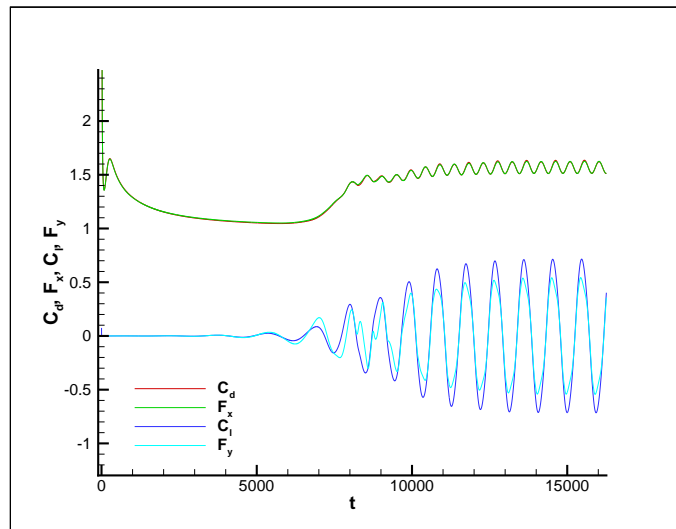


Figure 5.  $C_d$ ,  $F_x$ ,  $C_l$  and  $F_y$  with an stationed cylinder

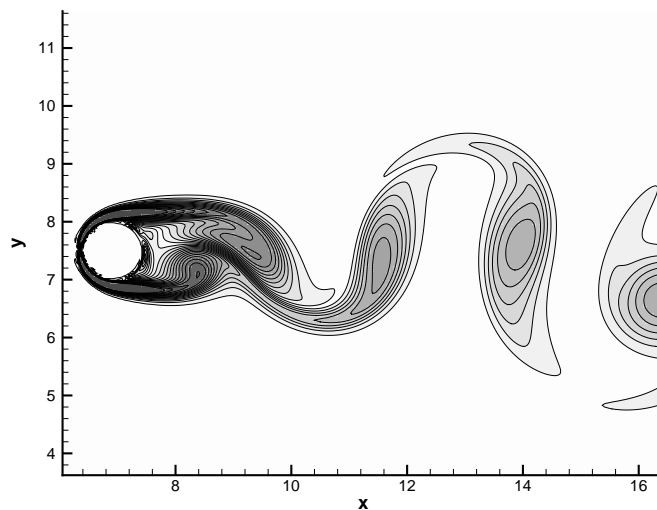


Figure 6. Vorticity contours for  $\omega = 0.5$  with an oscillating cylinder

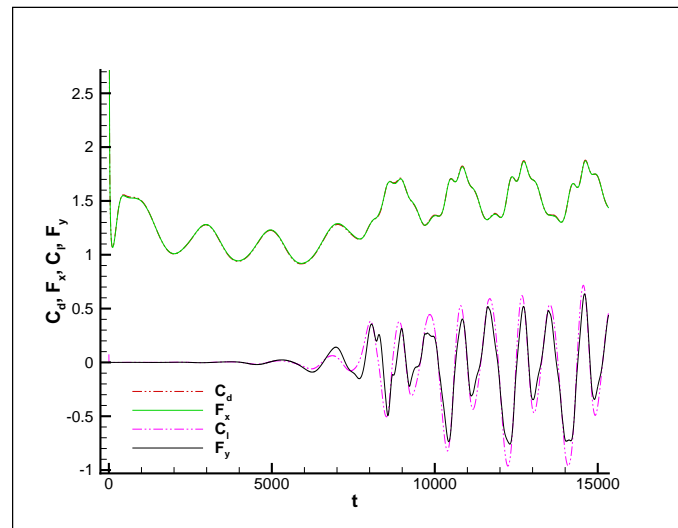


Figure 7.  $C_d$ ,  $F_x$ ,  $C_l$  and  $F_y$  for  $\omega = 0.5$  with an oscillating cylinder

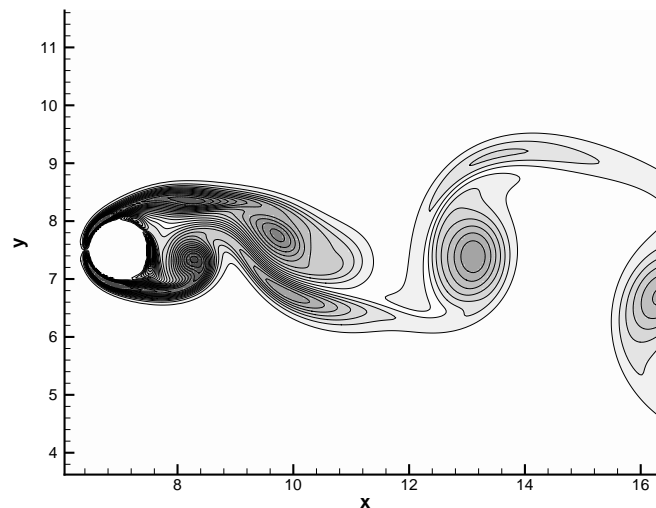


Figure 8. Vorticity contours for  $\omega = 1.5$  with an oscillating cylinder

The vorticity contours for  $Re = 190$  and frequency oscillation  $\omega = 1.5$  are shown in Fig. 8. The amplitude was also  $A = 0.2$ . In this figure it can be observed that the vortex shedding had a different pattern, and more vortices can be seen in the same space, if compared with Fig. 6. Figure 9 shows the results obtained for the  $C_d$ ,  $F_x$ ,  $C_l$  and  $F_y$ . It can be observed that the  $C_d$  and  $F_x$  have the same result while  $C_l$  and  $F_y$  showed some differences. Here it can be seen that the coefficients have a different frequency, showing that the lock-in phenomena has occurred, as expected by experiments of Griffin and Ramberg (1976).

Figure 10 shows the vorticity contours for  $Re = 190$  and frequency oscillation  $\omega = 2.0$ . The amplitude in this case was kept the same used for previous results ( $A = 0.2$ ). The vortex shedding pattern with this frequency is different from the previous results. This wake is formed by a pair of co-rotating vortices that are delivered each time the cylinder changes the moving direction. The values of  $C_d$ ,  $F_x$ ,  $C_l$  and  $F_y$  are shown in Fig. 11 Here, again, the values of  $C_l$  and  $F_y$  presented some differences. The frequency of the coefficients can again show the lock-in phenomena. This was expected for this frequency (Griffin and Ramberg, 1976).

For the oscillation frequency  $\omega = 3.0$ , a complex vortex street formation was found, as it can be observed in Fig.12. Near the cylinder the formation of two vortices with opposite signs occurs. These vortices in each side of the cylinder merge with the next vortex, developing new large-scale vortices. Figure 13 shows the  $C_d$ ,  $F_x$ ,  $C_l$  and  $F_y$  for oscillation frequency  $\omega = 3.0$ . The lock-in phenomena do not occur for this oscillation frequency.

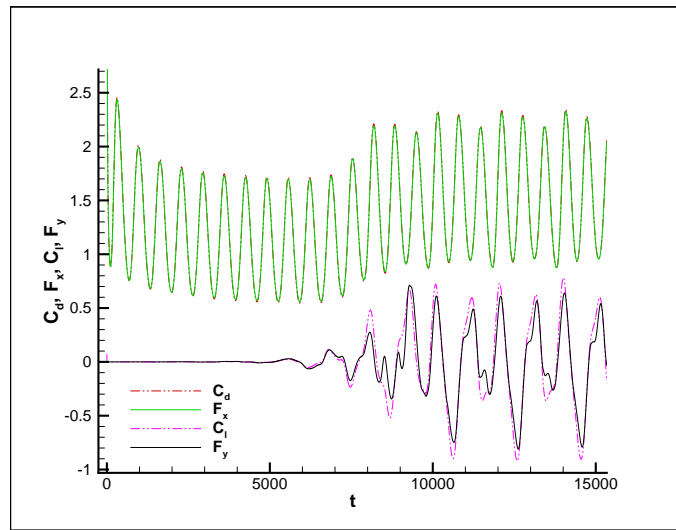


Figure 9.  $C_d$ ,  $F_x$ ,  $C_l$  and  $F_y$  for  $\omega = 1.5$  with an oscillating cylinder

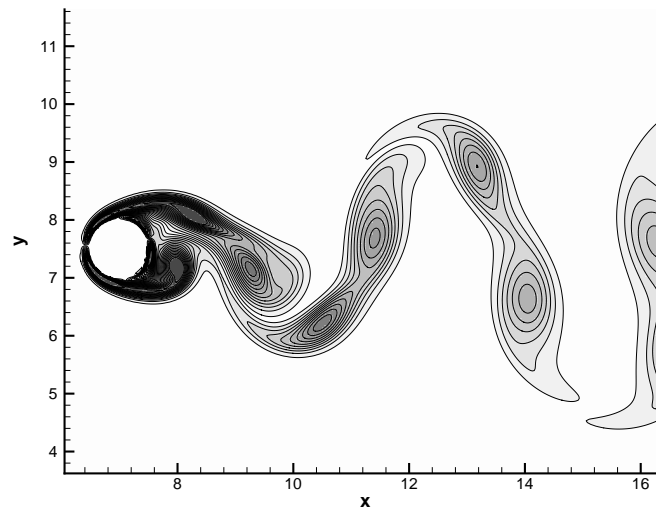


Figure 10. Vorticity contours for  $\omega = 2.0$  with an oscillating cylinder

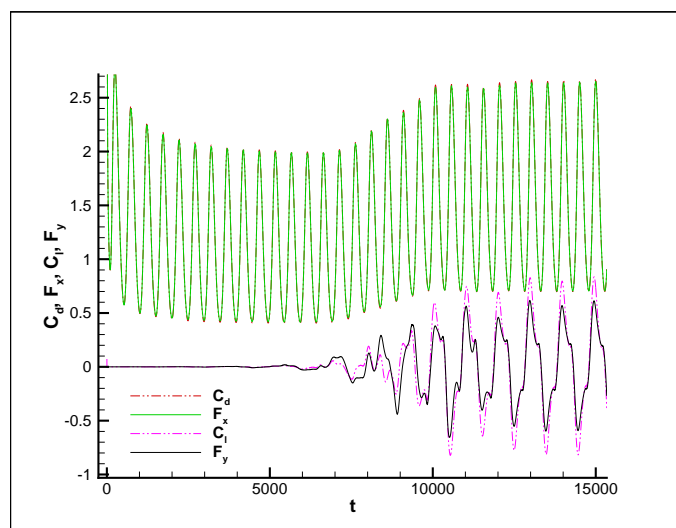


Figure 11.  $C_d$ ,  $F_x$ ,  $C_l$  and  $F_y$  for  $\omega = 2.0$  with an oscillating cylinder

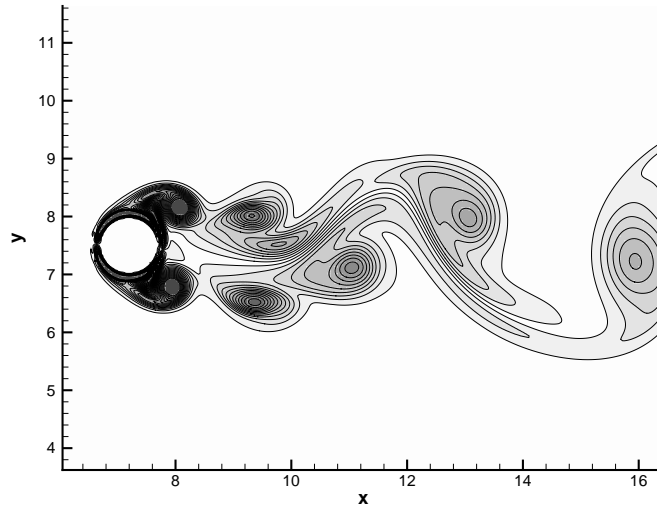


Figure 12. Vorticity contours for  $\omega = 3.0$  with an oscillating cylinder

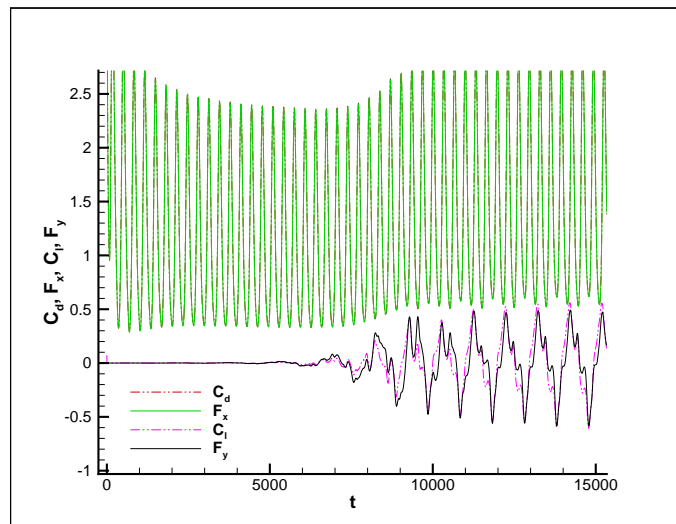


Figure 13.  $C_d, F_x, C_l$  and  $F_y$  for  $\omega = 3.0$  with an oscillating cylinder



#### 4. CONCLUSIONS

In the present work a numerical simulation of a flow over a cylinder was performed. An immersed boundary method was adopted, enabling the use of regular meshes, reducing the computational effort. The governing equations were written in vorticity-velocity formulation. The spatial derivatives were calculated by high order finite difference schemes. The time integration was performed by a fourth order Runge-Kutta scheme. A control volume was implemented and the lift and drag coefficients obtained were compared with the forcing terms of the governing equations.

The results obtained for the drag and lift coefficients for  $Re = 20$  and  $Re = 40$  simulations were in good agreement with previous numerical / experimental works. The results of vorticity contour of the simulations with an oscillating cylinder showed the occurrence of the lock-in phenomena and that this phenomena can also be shown by the drag and lift coefficients.

#### 5. ACKNOWLEDGEMENTS

The authors acknowledges Prof. Marcos Aurélio Ortega (ITA) and Prof. Jorge Silvestrini (PUCRS) for their help in implementing the control volume method.

#### 6. REFERENCES

- Braza, M., Chassaing, P. and Minh, H.H., 1986 "Numerical study and physical analysis of the pressure and velocity fields in the near wake of a circular cylinder", *Journal of Fluid Mechanics*, Vol.165, pp. 79-130.
- Góis, E.R.C and Souza, L.F., 2006, "Estudo numérico do escoamento em torno de um cilindro oscilante utilizando a técnica das fronteiras imersas", *Congresso Nacional de Matemática aplicada e Computacional*, Campinas, Brazil.
- Góis, E.R.C and Souza, L.F., 2007, "Numerical study of lock-in phenomena in 2D flow over a cylinder", *Proceedings of the 12th International symposium on Dynamic Problems of Mechanics*, Ilhabela, Brazil.
- Griffin, O.M. and Ramberg, S.E., 1976 "Vortex shedding from a cylinder vibrating in line with an incident uniform flow", *Journal of Fluid Mechanics*, Vol.75, pp. 257-271.
- Gu W., Chyu C. and Rockwell D., 1994, "Timing of vortex formation from an oscillating cylinder", *Phys. Fluids*, vol. 11, pp. 3677-3682.
- Kloker M., 1998, "A Robust High-Resolution Split-Type Compact FD Scheme for Spatial Direct Numerical Simulation of Boundary-Layer Transition", *Applied Scientific Research*, vol. 59, pp 353-377.
- Peskin, C. S., 1972, "Flow Patterns Around Heart Valves: A Numerical Method", *J. Computational Physics*, Vol. 10, pp. 252-271.
- Souza L. F. and Mendonça M. T. and Medeiros M. A. F., 2005, "The advantages of using high-order finite differences schemes in laminar-turbulent transition studies", *Int. Journal for Numerical Methods in Fluids*, vol. 48, pp. 565-592.

#### 7. Responsibility notice

The authors are the only responsible for the printed material included in this paper.